Nedd9 restrains renal cystogenesis in *Pkd1*$^{-/-}$ mice

Anna S. Nikonova[a], Olga V. Plotnikova[a,1], Victoria Serzhanova[a], Andrey Efimov[b], Igor Bogush[a], Kathy Q. Cai[b], Harvey H. Hensley[a], Brian L. Egleston[a], Andres Klein-Szanto[b], Tamina Seeger-Nukpezah[a,2], and Erica A. Golemis[a,3]

Programs in [a]Developmental Therapeutics and [b]Cancer Biology, Fox Chase Cancer Center, Philadelphia, PA 19111

Edited by Kathryn V. Anderson, Sloan–Kettering Institute, New York, NY, and approved July 30, 2014 (received for review March 25, 2014)

Mutations inactivating the cilia-localized Pkd1 protein result in autosomal dominant polycystic kidney disease (ADPKD), a serious inherited syndrome affecting ∼1 in 500 people, in which accumulation of renal cysts eventually destroys kidney function. Severity of ADPKD varies throughout the population, for reasons thought to involve differences both in intragenic *Pkd1* mutations and in modifier alleles. The scaffolding protein NEDD9, commonly dysregulated during cancer progression, interacts with Aurora-A (AURKA) kinase to control ciliary resorption, and with Src and other partners to influence proliferative signaling pathways often activated in ADPKD. We here demonstrate Nedd9 expression is deregulated in human ADPKD and a mouse ADPKD model. Although genetic ablation of Nedd9 does not independently influence cystogenesis, constitutive absence of *Nedd9* strongly promotes cyst formation in the tamoxifen-inducible *Pkd1fl/fl;Cre/Esr1*$^{+}$ mouse model of ADPKD. This cystogenic effect is associated with striking morphological defects in the cilia of *Pkd1*$^{-/-}$*;Nedd9*$^{-/-}$ mice, associated with specific loss of ciliary localization of adenylase cyclase III in the doubly mutant genotype. Ciliary phenotypes imply a failure of Aurora-A activation: Compatible with this idea, *Pkd1*$^{-/-}$*;Nedd9*$^{-/-}$ mice had ciliary resorption defects, and treatment of *Pkd1*$^{-/-}$ mice with a clinical Aurora-A kinase inhibitor exacerbated cystogenesis. In addition, activation of the ADPKD-associated signaling effectors Src, Erk, and the mTOR effector S6 was enhanced, and Ca^{2+} response to external stimuli was reduced, in *Pkd1*$^{-/-}$*;Nedd9*$^{-/-}$ versus *Pkd1*$^{-/-}$ mice. Together, these results indicated an important modifier action of Nedd9 on ADPKD pathogenesis involving failure to activate Aurora-A.

HEF1 | ganetespib | STA-2842

Autosomal dominant polycystic kidney disease (ADPKD) is one of the most common inherited kidney diseases, affecting 600,000 people in the United States (1). The disease is predominantly characterized by the development and enlargement of renal cysts, as well as extrarenal systems that commonly include sporadic cysts in the liver, seminal vesicles (in males), and pancreas; hypertension; and vascular manifestations associated with aneurysms (2). There is no specific treatment available that can prevent ADPKD progression toward end-stage renal disease (ESRD), associated with a requirement for renal transplant or dialysis. Given the time of onset of ADPKD varies more than two decades in affected families, and the disease can progress in an indolent or aggressive manner, identifying modifier genes that increase or decrease the severity of ADPKD symptoms would be clinically valuable.

ADPKD arises from mutational inactivation of polycystin 1 and 2 (PC1 and PC2), encoded by polycystic kidney disease (PKD) 1 and PKD2, two heterodimerizing transmembrane proteins that transmit extracellular mechanical and molecular cues by increasing cellular Ca^{2+} uptake and association with intracellular signaling partners. Multiple signaling pathways are compromised in ADPKD. Observed defects including elevated activity of receptor tyrosine kinases (EGFR, IGF1R, and VEGFR); activation of the Ras-Raf-ERK proliferative signaling; elevated activity of the Src, PKA, mTOR, and S6 kinases; and altered levels of intracellular cAMP and Ca^{2+}, affecting numerous second messenger pathways (2). PC1 and PC2 function as a heterodimer displayed on the cell membrane of the primary cilium, an organelle that protrudes like an antenna from many cells. For this reason, and because defects in the cilium per se can result in renal cystic syndromes that have some features of ADPKD (3), ADPKD is classified among the ciliopathies.

NEDD9 (also known as HEF1 and Cas-L) is a scaffold for cell signaling interactions that govern cell attachment and migration (4, 5), survival (6), mitogenic signaling and cell cycle control (7–10), and ciliary resorption (11, 12). To date, NEDD9 has been most studied in the context of cancer, because deregulated expression of NEDD9 accompanies and promotes metastasis in a large and growing number of cancer types, whereas genetic ablation of NEDD9 has a significant modifier function for tumor initiation and progression (8, 13, 14). A particularly interesting feature of NEDD9 action in cancer is that both overexpression and loss of function have been found to be tumor promoting different cellular contexts, likely because either form of disruption of its scaffolding action impairs downstream processes.

Importantly, NEDD9 interacts directly with a number of signaling proteins that are directly relevant to functions disrupted in ADPKD. NEDD9 binds and activates SRC, regulating cell migration and attachment (15–17). NEDD9 supports the activity of the EGFR effector cascade, binding directly to the EGFR effector Shc1 (7, 8). Nedd9 binds and is required for activity of Aurora-A kinase: The loss of interactions between these proteins induces genomic abnormalities and centrosomal defects (18, 19), causes loss of ciliary resorption (12), and influences PKD2-associated signaling (20, 21). Based on these and other findings, we have hypothesized that NEDD9 expression might have a role

Significance

This study uses mouse models for the first time to our knowledge to identify that NEDD9, a nonenzymatic scaffolding protein that is commonly amplified in cancer, has an important restraining function for the development of renal cysts in autosomal dominant polycystic kidney disease (ADPKD). In the absence of NEDD9, failure to activate Aurora-A kinase causes multiple abnormalities in cilia, intensifying the effect of genetic deficiency of mutations in the polycystic kidney disease (PKD) 1 gene, the most common cause of PKD. As important implications, clinical inhibitors of Aurora-A also intensified ADPKD induced by mutation of *PKD1*, suggesting caution in use of these agents, whereas recently reported polymorphisms in Nedd9 may contribute to the genetic heterogeneity of ADPKD presentation in affected families.

Author contributions: A.S.N. and E.A.G. designed research; A.S.N., O.V.P., V.S., A.E., I.B., K.Q.C., and T.S.-N. performed research; H.H.H. contributed new reagents/analytic tools; A.S.N., O.V.P., I.B., K.Q.C., B.L.E., and A.K.-S. analyzed data; A.S.N., B.L.E., A.K.-S., and E.A.G. wrote the paper.

The authors declare no conflict of interest.

This article is a PNAS Direct Submission.

[1]Present address: Department of Biochemistry and Molecular Biology, Monash University, Clayton, Victoria 3800, Australia.

[2]Present address: Department of Internal Medicine, Center for Integrated Oncology, University Hospital of Cologne, 50931 Cologne, Germany.

[3]To whom correspondence should be addressed. Email: erica.golemis@fccc.edu.

This article contains supporting information online at www.pnas.org/lookup/suppl/doi:10.1073/pnas.1405362111/-/DCSupplemental.

in controlling signaling processes associated with renal cystogenesis. The results reported here indicate a striking modifier function of NEDD9 and its effector Aurora-A on the process of cystogenesis, mediated through regulation of both ciliary and nonciliary signaling.

Results

***Nedd9* Expression Is Elevated in Renal Cysts.** We first examined NEDD9 expression in kidney sections of patients diagnosed with PKD. Immunohistochemical analysis of primary human kidney specimens detected intense NEDD9 staining in the epithelial lining of cysts. Less intense staining was also seen in cells of the proximal and distal convoluted tubules, and in the collecting ducts, but not in the glomerulus (Fig. 1*A*). This expression pattern is similar to that we identified for AURKA (20) and reported for PC2 (22). *Pkd1fl/fl;Cre/Esr1*$^{+}$ mice induced with tamoxifen at postnatal day (P)2 and P3 (referred to as *Pkd1*$^{-/-}$ mice) develop renal cysts with 100% penetrance, with kidney highly cystic by P15 (23, 24). Although no antibodies exist for immunohistochemical analysis of Nedd9 in mouse tissue, quantification from Western blots suggested that expression of Nedd9 was elevated in the early cystic (P10) kidneys of *Pkd1*$^{-/-}$ versus wild-type mice (Fig. 1*B*), encouraging further study in this model.

***Nedd9* Restrains Renal Cystogenesis in *Pkd1*$^{-/-}$ Mice.** To evaluate potential functions of Nedd9 in cystogenesis, we compared relative cystogenesis in *Pkd1*$^{-/-}$, *Nedd9*$^{-/-}$, and *Pkd1*$^{-/-}$;*Nedd9*$^{-/-}$ mice. *Nedd9*$^{-/-}$ are typically viable and fertile, with limited defects appearing in mice >1 y of age (25). Analysis of kidneys collected at P10 revealed a significant increase in kidney size and a much more extensive cystogenesis in *Pkd1*$^{-/-}$;*Nedd9*$^{-/-}$ relative to *Pkd1*$^{-/-}$ mice (Fig. 1 *C–F* and Fig. S1*A*). In contrast, mice with a *Nedd9*$^{-/-}$ genotype were comparable to *wt* mice in kidney size and absence of cysts, indicating a modifier rather than a primary function in cyst generation. Together these data indicated a physiological role of Nedd9 in control of cyst formation in the context of an initiating lesion in *Pkd1*. In preliminary studies to compare genotypes at P15, when cystogenesis is well advanced in *Pkd1*$^{-/-}$ mice, we found that *Pkd1*$^{-/-}$;*Nedd9*$^{-/-}$ mice did not survive to P15, with mortality commencing at P11.

Histopathological analysis of P10 renal tissue with markers of proximal and distal convoluted tubules, collecting ducts, and the medullary thick ascending loops of Henle (Fig. S1 *B* and *C*) indicated that cysts originated from all three compartments in both *Pkd1*$^{-/-}$ and *Pkd1*$^{-/-}$;*Nedd9*$^{-/-}$ mice. The larger cysts in each case associated with markers for collecting ducts and the loops of Henle, regardless of genotype. Ki67 staining followed by quantification of Ki67-positive cells lining tubules versus cysts in P10 kidneys indicated a nonstatistically significant trend toward a higher level of proliferating cells in the tubules of *Pkd1*$^{-/-}$;*Nedd9*$^{-/-}$ mice relative to *wt*, *Pkd1*$^{-/-}$, or *Nedd9*$^{-/-}$ tissue (Fig. 1 *G* and *H*). Analysis of the Ki67 staining in the early cysts of the *Pkd1*$^{-/-}$ and *Pkd1*$^{-/-}$;*Nedd9*$^{-/-}$ mice showed similar levels of proliferation in both genotypes, in each case significantly elevated relative to wt or *Nedd9*$^{-/-}$ kidneys (Fig. 1 *G* and *H*). Staining of cells for cleaved caspases, a marker of apoptosis, identified fewer than 1% of cells positive in all genotypes, indicating that this process was not significantly related to *Pkd1*$^{-/-}$-dependent cystogenesis or affected by *Nedd9* status.

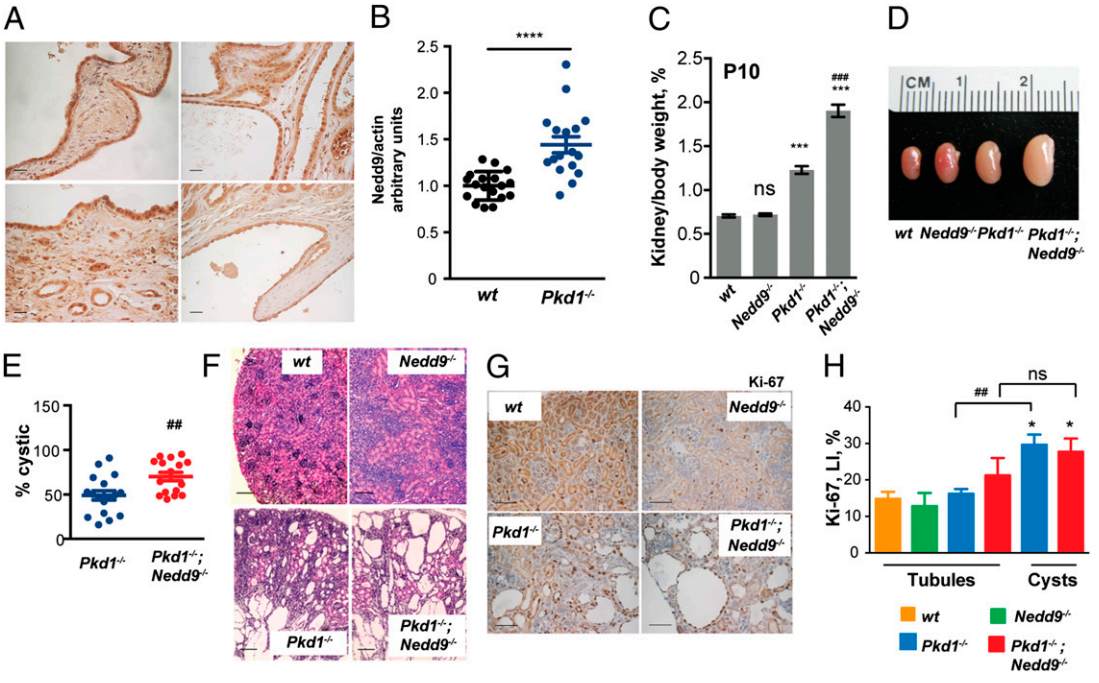

Fig. 1. The Nedd9$^{-/-}$ genotype enhances cyst formation in an early onset, inducible *Pkd1*$^{-/-}$ mouse model. (*A*) Immunohistochemical analysis of Nedd9 expression in primary tissue from patients diagnosed with PKD. (*B*) Relative abundance of Nedd9 protein level detected by Western blot in *wt* ($n = 19$) and *Pkd1*$^{-/-}$ ($n = 17$) kidney lysates, normalized to β-actin and quantified by ImageJ. ****$P \leq 0.0001$. (*C*) Kidney weight to body weight ratio for mice of the indicated genotypes at P10. ns, not significant; ***$P \leq 0.001$ compared with *wt*; $^{\#\#\#}$, $P < 0.001$ compared with Pkd1$^{-/-}$. (*D*) Examples of P10 kidneys of *wt*, *Nedd9*$^{-/-}$, *Pkd1*$^{-/-}$, and *Pkd1*$^{-/-}$;*Nedd9*$^{-/-}$ mice in which *Pkd1* was inactivated by tamoxifen treatment on P2. (*E*) Quantitation of percent of kidney filled with cysts in *Pkd1*$^{-/-}$ and *Pkd1*$^{-/-}$;*Nedd9*$^{-/-}$ animals at P10. $^{\#\#}$, $P \leq 0.01$ compared with *Pkd1*$^{-/-}$. Data are expressed as mean ± SEM. (*F*) Representative H&E staining of kidneys harvested 10 d after Pkd1 inactivation was induced at P2. (*G*) KI-67 stained sections of *wt*, *Nedd9*$^{-/-}$, *Pkd1*$^{-/-}$, and *Pkd1*$^{-/-}$;*Nedd9*$^{-/-}$ kidneys on P10; nuclear staining is specific. LI, labeling index. (*H*) Quantitation of KI-67 staining of *wt*, *Nedd9*$^{-/-}$, *Pkd1*$^{-/-}$, and *Pkd1*$^{-/-}$;*Nedd9*$^{-/-}$ kidneys on P10, separating values for tubules and ducts versus cysts. *$P \leq 0.05$ compared with *wt* tubules. $^{\#\#}P \leq 0.01$ compared with *Pkd1*$^{-/-}$; ns, not significant. Data are expressed as mean ± SEM. (Scale bars: *A*, 25 μm; *F*, 100 μm; *G*, 25 μm.) (Magnification: *A*, 100×; *F*, 20×; *G*, 40×.)

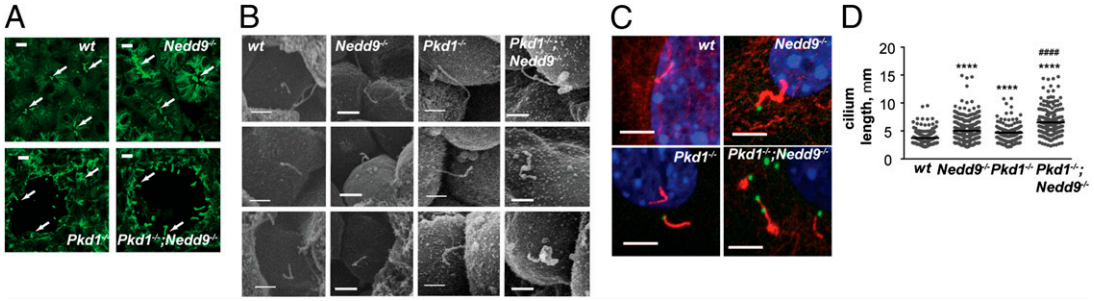

Fig. 2. Cilia are lengthened, irregular, and resistant to resorption in *Pkd1*$^{-/-}$;*Nedd9*$^{-/-}$ kidneys and kidney cells. (*A*) Acetylated α-tubulin staining to visualize cilia in kidney sections from *wt*, *Nedd9*$^{-/-}$, *Pkd1*$^{-/-}$, and *Pkd1*$^{-/-}$;*Nedd9*$^{-/-}$ mice. (*B*) Scanning electron microscopy analysis of primary cilia in kidneys of the indicated genotypes, representative images. See also Fig. S1. (*C*) Antibodies to acetylated α-tubulin (red) indicate cilia, and to γ-tubulin (green) indicate centrosomes and basal bodies, whereas DAPI (blue) indicates DNA in primary kidney cells isolated from *wt*, *Nedd9*$^{-/-}$, *Pkd1*$^{-/-}$, and *Pkd1*$^{-/-}$;*Nedd9*$^{-/-}$ P10 kidneys. (*D*) Quantitation of data shown in *C*, cilia length. Average ciliary length was 3.7 μM (*wt*), 5.0 μM (*Nedd9*$^{-/-}$), 4.7 μM (*Pkd1*$^{-/-}$) and 6.5 μM (*Pkd1*$^{-/-}$;*Nedd9*$^{-/-}$). $n = 150$ cells for each genotype. $^{****}P \leq 0.0001$ compared with wt; $^{\#\#\#\#}P \leq 0.0001$ compared with *Pkd1*$^{-/-}$. (Scale bars: *A*, 2 μm; *B* and *C*, 5 μm.) (Magnification: *A*, 40×; *B*, 4000×; *C*, 120×.)

Ciliary and Calcium Signaling Defects in *Pkd1*$^{-/-}$;*Nedd9*$^{-/-}$ Mice. Defects in ciliation are associated with cystogenesis, and NEDD9 control of Aurora-A can influence ciliary dynamics (12). In P10 kidney tissue (Fig. 2 *A* and *B* and Fig. S2) and primary kidney cells collected from P10 mice (Fig. 2 *C* and *D*) from *wt*, *Nedd9*$^{-/-}$, *Pkd1*$^{-/-}$, and *Pkd1*$^{-/-}$;*Nedd9*$^{-/-}$ mice, immunofluorescence and electron micrographs demonstrate that in all mutant genotypes, cilia were significantly lengthened relative to wild type, with this phenotype particularly pronounced in the *Nedd9*$^{-/-}$ and *Pkd1*$^{-/-}$;*Nedd9*$^{-/-}$ genotypes. Strikingly, the cilia observed in *Pkd1*$^{-/-}$;*Nedd9*$^{-/-}$ kidneys in vivo were not only lengthened, but also were commonly abnormally shaped, with thickened bulges along the length of the cilium. These results suggested the possibility of a defect in ciliary trafficking. We examined localization of a number of ciliary proteins, including intraflagellar transport protein IFT88, a component of the IFT-B complex (26), INPP5E and ARL13B, membrane-associated proteins associated with the ciliopathy Joubert's syndrome (27), and the ciliary protein adenylate cyclase III (ACIII), which catalyzes the production of cAMP, is abnormally regulated in ADPKD (28), and is excluded from the cilia of fibroblasts from individuals with familial nephronophthisis-like cystic syndromes (29). IFT88, INPP5E, and ARL13B were comparably localized in cilia regardless of Pkd1 or Nedd9 genotype (Fig. S3 *A*–*C*). In contrast, ACIII showed a striking exclusion from the cilia in *Pkd1*$^{-/-}$;*Nedd9*$^{-/-}$ cells (Fig. 3*A*), suggesting a selective trafficking deficit. Impaired cilia have also been shown to affect the functionality of the vasopressin receptor V2R, contributing to the pathogenesis of cystic kidney diseases (30). Consistent with this idea, transient stimulation with arginine vasopressin (AVP) resulted in a significantly depressed response in *Pkd1*$^{-/-}$;*Nedd9*$^{-/-}$ cells versus all other genotypes (Fig. 3*B*).

Nedd9 binding and activation of Aurora-A is required for ciliary resorption (12, 31), and we have observed that Aurora-A expression is elevated in the cystic tissue of patients with ADPKD (20). These results suggested the hypothesis that defects in Aurora-A activation at cilia might underlie the observed trafficking and morphological defects. Western blot and immunohistochemical analysis showed comparable levels of

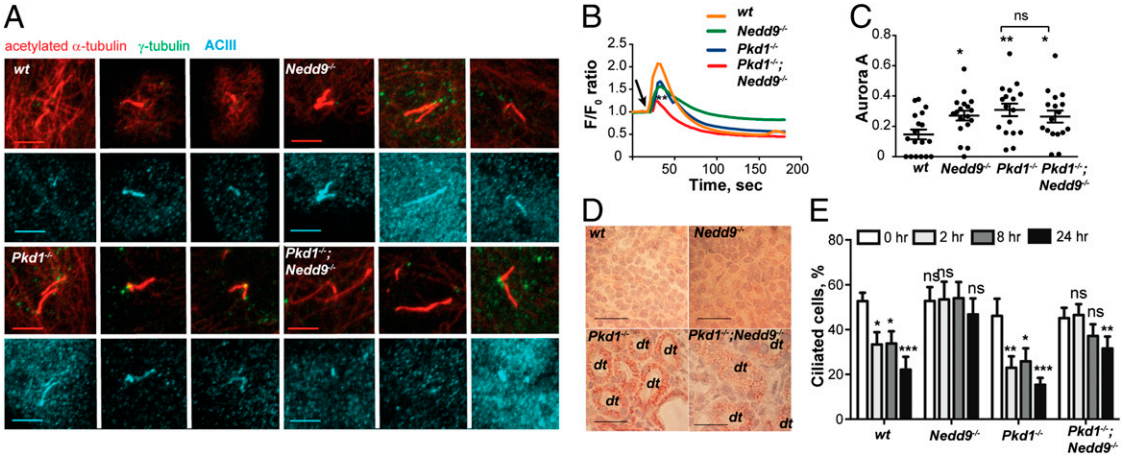

Fig. 3. Defects in ciliary trafficking and calcium response are exacerbated in *Pkd1*$^{-/-}$;*Nedd9*$^{-/-}$ kidney cells. (*A*) Immunofluorescence with antibodies to IFT88 (*A*) and ACIII (*B*) shows localization in cilia based. Acetylated α-tubulin (red) and γ-tubulin (green) indicate axoneme and basal body. (*C*) Fluorescence of cells preloaded with 5 μM Fluo-4 AM was measured before and after addition of AVP (indicated by arrow). Data are plotted as the F/F_0 ratio, where F_0 and F are fluorescence intensity measured before and after AVP addition, respectively. The mean increase in amplitude (± SEM) of AVP-induced cytoplasmic Ca^{2+} transients was calculated from $n > 25$ cells in each of three experiments. $^{*}P \leq 0.05$, $^{**}P \leq 0.01$, compared with *wt*. (*D*) Quantification of Western blot analysis shows expression of Aurora-A in P10 kidney lysates. $^{*}P \leq 0.05$, $^{**}P = 0.0015$, compared with *wt*; ns, not significant. (*E*) Aurora-A staining of kidney sections from *wt*, *Nedd9*$^{-/-}$, *Pkd1*$^{-/-}$, and *Pkd1*$^{-/-}$;*Nedd9*$^{-/-}$ mice. (*F*) Percentage of ciliated cells 0, 2, 8, and 24 h after serum induction of ciliary disassembly in primary kidney cells isolated from P10 kidneys of *wt*, *Nedd9*$^{-/-}$, *Pkd1*$^{-/-}$, and *Pkd1*$^{-/-}$;*Nedd9*$^{-/-}$ mice. $^{*}P \leq 0.05$; $^{**}P \leq 0.01$; $^{***}P \leq 0.001$; ns, not significant compared with 0 h. All data are expressed as mean ± SEM. (Scale bars: *A*, 5 μm; *D*, 25 μm.) (Magnification: *A*, 400×; *D*, 100×.)

total Aurora-A in *wt* and *Nedd9*$^{-/-}$ P10 kidneys, and a more heterogeneous pattern in *Pkd1*$^{-/-}$ and *Pkd1*$^{-/-}$;*Nedd9*$^{-/-}$ kidneys, reflecting slight elevation of total Aurora-A expression in a subset of kidneys from each genotype (Fig. 3 *C* and *D*). At this time, no antibodies exist that reliably report T^{288} phosphorylation (a typical gauge of activation) of murine Aurora-A. However, analysis of ciliary resorption patterns confirm deficiency in ciliary resorption in *Pkd1*$^{-/-}$;*Nedd9*$^{-/-}$ versus *Pkd1*$^{-/-}$ primary kidney cells, particularly at earlier G_1 time points (Fig. 3*E*), compatible with impaired Aurora-A activity.

Elevation of Procystogenic Signaling in *Pkd1*$^{-/-}$;*Nedd9*$^{-/-}$ Mice. Beyond the effects on cilia, in studies of cancer cells, Nedd9 has been demonstrated to influence signaling relevant to cell proliferation and migration, involving EGFR (7), Src (32), and their effectors (8). Given the relevance of these pathways to ADPKD (2), we analyzed P10 kidneys to examine changes in these pathways. At P10, the activation of proliferation-associated kinases typically seen in ADPKD was not yet significant in *Pkd1*$^{-/-}$ mice. However, Western blot analysis revealed a significant elevation in the expression and activation of the Src, S6, and ERK kinases in *Pkd1*$^{-/-}$;*Nedd9*$^{-/-}$ P10 mice (Fig. 4 *A*–*C*). In detailed analysis of individual mice (Fig. 4 *D* and *E*), activation of Src and S6 (levels of phospho-Y^{416}-Src and phospho-S^{235}/S^{236}-S6) strongly correlated in the context of the *Pkd1*$^{-/-}$;*Nedd9*$^{-/-}$ genotype.

Exclusion of Mechanisms for Nedd9 Influence on Cystogenesis. Our work also excluded several potential explanations for ways in which absence of *Nedd9* might contribute to cystogenesis, either because the phenotype was seen in *Nedd9*$^{-/-}$ mice (which did not develop cysts) at least as strongly as in *Pkd1*$^{-/-}$ mice, or because *Pkd1*$^{-/-}$;*Nedd9*$^{-/-}$ did not have a stronger phenotype than *Pkd1*$^{-/-}$ mice. These experiments included control of rate of multiciliation (Fig. S4*A*) or supernumerary centrosomes (Fig. S4*B*), or changes affecting in vitro renal cell proliferation (Fig. S4*C*) or cell cycle compartmentalization (Fig. S4*D*). In regard to signaling defects, analysis of expression and activation of EGFR, AKT, CDK1, and FAK (Fig. S5) did not reveal genotype-specific correlations informative for cystogenic phenotypes.

***Nedd9* Limits Renal Cystogenesis in Older *Pkd1*$^{-/-}$ Mice with Sporadic Onset PKD.** If loss of *Pkd1* is induced in *Pkd1fl/fl;Cre/Esr1*$^{+}$ mice after P12–14, instead of a 100% penetrant, rapid onset disease, cystogenesis occurs in a sporadic manner at 4–6 mo, with a phenotype that closely resembles human ADPKD (23). To ensure *Nedd9*$^{-/-}$ phenotypes were not specific to the early induction, early onset model of cystogenesis, we also analyzed the consequences of a Nedd9-null genotype after inducing Pkd1 loss by administering tamoxifen at P35 and P36. We used magnetic resonance imaging () (Fig. S6*A*) to monitor kidney growth and cyst formation at monthly intervals beginning at month 4. Quantification of this data (Fig. S6 *B* and *C*) and direct analysis of tissue upon euthanasia at 6.5 mo (Fig. S6 *D*–*G*) again indicated that in conjunction with loss of *Pkd1*, a *Nedd9*$^{-/-}$ genotype strongly enhanced kidney growth and cystogenesis, and slightly enhanced KI-67 staining in dilated tubules and cysts (Fig. S6*G*). KI-67 staining was negligible in the normal tubules of *wt* and *Nedd9*$^{-/-}$ adult mice (Fig. S6*G*). Interestingly, although the late onset, *Pkd1fl/fl;Cre/Esr1*$^{+}$ model is also prone to extensive formation of hepatic cysts (24), this process was not affected by *Nedd9*-null status (Fig. S6*H*), in accord with prior reports of low Nedd9 expression in the liver (33).

Direct Implication of Aurora-A Inhibition in Cystogenesis and Ciliary Defects. In sum, these data suggested that loss of Aurora-A activation in *Pkd1*$^{-/-}$;*Nedd9*$^{-/-}$ mice was responsible for cystogenesis. To test this idea, we induced loss of *Pkd1* with tamoxifen treatment at P35 and P36, then dosed mice with vehicle or the Aurora-A inhibitor MLN8237 (alisertib) from ages 4–6 mo, while observing kidney growth and cyst formation by MRI (Fig. 5*A* and Fig. S7 *A* and *B*). Alisertib significantly potentiated the rate of cyst and kidney growth in a *Pkd1*$^{-/-}$ genetic background. Notably, cilia from *Pkd1*$^{-/-}$ mice treated with alisertib were visibly lengthened relative to vehicle-treated mice, and some had bulges (Fig. S7*C*). We then treated primary kidney cells from *wt*, *Nedd9*$^{-/-}$, *Pkd1*$^{-/-}$, and *Pkd1*$^{-/-}$;*Nedd9*$^{-/-}$ mice with alisertib for 48 h during serum starvation and cilia formation. Alisertib treatment lengthened cilia in *wt* and *Pkd1*$^{-/-}$ cells, but did not further increase the length of cilia in *Nedd9*$^{-/-}$ or *Pkd1*$^{-/-}$;*Nedd9*$^{-/-}$ cells (Fig. 5*B*), implying redundant function with loss of *Nedd9*. Alisertib also blocked serum-induced ciliary resorption in all genotypes (Fig. 5*C*), and induced a higher frequency of malformed cilia, particularly in the *wt* genotype (Fig. S7*D*). In *Pkd1*$^{-/-}$ cells, although some bulging was seen, the predominant phenotype was multiciliation (Fig. S7*D*). However, ACIII was selectively absent in cilia of alisertib-treated cells of the *Pkd1*$^{-/-}$ genotype, matching the double knockout (Fig. S7*E*).

In contrast, 2 h of treatment in serum-free medium with the Aurora-A activating compound anacardic acid (34) induced nearly total resorption of cilia in *wt* and *Pkd1*$^{-/-}$ cells, but did not cause resorption of cilia in *Nedd9*$^{-/-}$ or *Pkd1*$^{-/-}$;*Nedd9*$^{-/-}$ cells, suggesting a potential additional requirement for Nedd9 in completing the resorption process (Fig. 5*D*). However, anacardic acid rapidly induced dramatic shortening of cilia in all genotypes (Fig. 5*E*), and the short residual cilia seen in anacardic acid-treated *Nedd9*$^{-/-}$ or *Pkd1*$^{-/-}$;*Nedd9*$^{-/-}$ cells were morphologically more normal than those in vehicle-treated cells (Fig. S7*F*). Together,

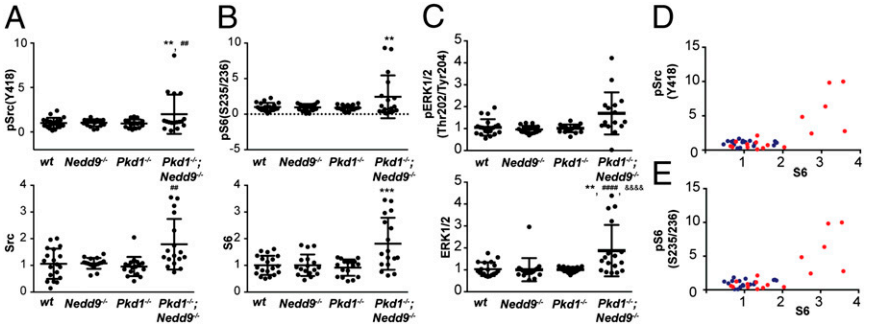

Fig. 4. *Nedd9*$^{-/-}$ regulation of signaling activation in mouse kidneys. (*A*–*C*) Quantification of Western blot analysis shows expression and activation levels of total and phosphorylated (active) Src (*A*), S6 (*B*), and ERK (*C*) in kidney lysates of the *wt* (n = 19), *Nedd9*$^{-/-}$ (n = 17), *Pkd1*$^{-/-}$ (n = 17), and *Pkd1*$^{-/-}$;*Nedd9*$^{-/-}$ (n = 17) genotypes. Data are expressed as mean ± SE. $^{**}P \le 0.01$, $^{***}P \le 0.001$, compared with *wt*; $^{\#\#}P \le 0.01$, $^{\#\#\#\#}$, $P \le 0.0001$ in comparison with *Pkd1*$^{-/-}$; $^{\&\&\&\&}P \le 0.0001$ in comparison with *Nedd9*$^{-/-}$. For phospho-Src, heterogeneity of *Pkd1*$^{-/-}$;*Nedd9*$^{-/-}$ is highly significant with respect to *wt*, *Nedd9*$^{-/-}$, and *Pkd1*$^{-/-}$; $P < 0.0001$ (in all cases). For total Src, heterogeneity of *Pkd1*$^{-/-}$;*Nedd9*$^{-/-}$ is significant with respect to *wt* ($P = 0.0369$) and *Nedd9*$^{-/-}$ ($P = 0.0005$). For phospho-Erk, heterogeneity of *Pkd1*$^{-/-}$;*Nedd9*$^{-/-}$ is highly significant with respect to *Pkd1*$^{-/-}$ ($P \le 0.0001$) and *Nedd9*$^{-/-}$ ($P = 0.0008$), but not to *wt* ($P = 0.7858$). For total Erk1/2, heterogeneity of *Pkd1*$^{-/-}$;*Nedd9*$^{-/-}$ with respect to *wt*, *Nedd9*$^{-/-}$, and *Pkd1*$^{-/-}$ is highly significant ($P < 0.001$ in all cases). (*D*) Association between total S6 protein and pSrc^{Y418} level in *Pkd1*$^{-/-}$ ($P > 0.5$) and *Pkd1*$^{-/-}$*Nedd9*$^{-/-}$ animals ($P = 0.0036$). (*E*) Association between total S6 protein and pS6$^{S235/236}$ level in *Pkd1*$^{-/-}$ ($P > 0.5$) and *Pkd1*$^{-/-}$*Nedd9*$^{-/-}$ animals ($P = 0.0033$). Dots represent individual animals with *Pkd1*$^{-/-}$ (blue) and *Pkd1*$^{-/-}$*Nedd9*$^{-/-}$ (red) genotypes.

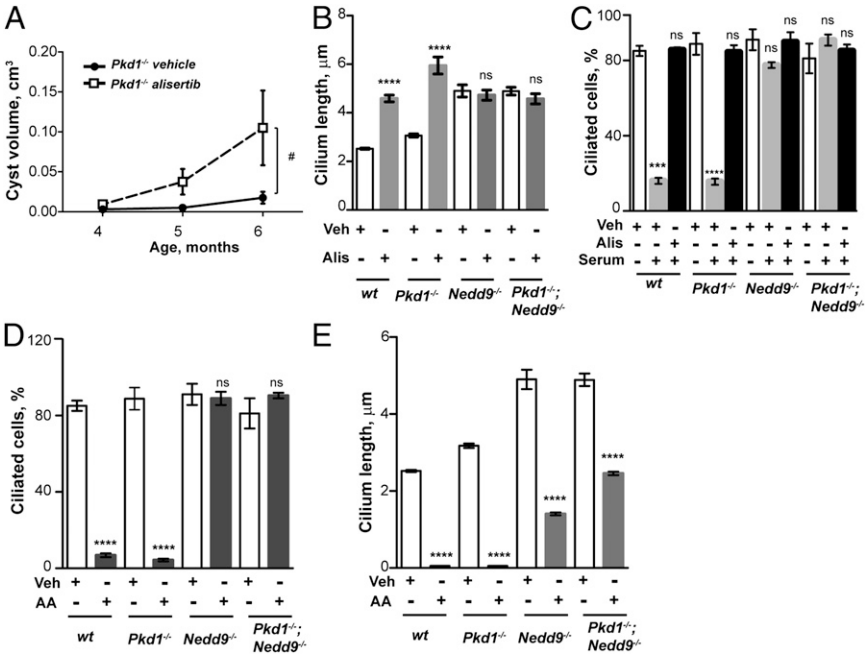

Fig. 5. Aurora-A inhibition promotes cystogenesis and ciliary defects. (*A*) Cyst volume in cubic centimeters in mice treated with alisertib or vehicle based on quantitation of MRI images; $*P \leq 0.043$, compared with *wt*. Data are expressed as mean ± SEM. (*B*) Length of cilia in micrometers after 48 h incubation in serum-free medium including DMSO (vehicle) or alisertib, quantification length. $****P <$ 0.0001 versus vehicle-treated. At least 150 cells were measured per genotype. (*C*) Frequency of ciliated cells in cultures maintained in no serum, or treated with 2 h of serum, with DMSO (vehicle) or alisertib as indicated. At least 750 cells were scored per genotype. $***P < 0.001$, $****P < 0.0001$, versus no serum control; ns, not significant. (*D*) Frequency of ciliated cells in cultures maintained in serum-free medium, with DMSO (vehicle) or anacardic acid as indicated. $****P < 0.0001$ versus vehicle control; ns, not significant. (*E*) Length of cilia in micrometers after 2 h in anacardic acid in serum-free medium; $***P < 0.001$ versus vehicle control. At least 150 cells were measured per genotype.

these data indicated Aurora-A activation is a critical effector of Nedd9 in regulation of cilia and cystogenesis, but does not completely phenocopy Nedd9, implying additional functions.

Discussion

Although Nedd9 has been much studied in the context of cancer (35), little is known about the role of this protein in other pathological conditions. Our data demonstrate that loss of *Nedd9* strongly enhances the kidney expansion and cystogenesis induced by the loss of *Pkd1* either before or after the P13 developmental switch (23), for the first time, to our knowledge, defining *Nedd9* as a candidate modifier gene for human ADPKD. Based on examination of multiple candidate *Nedd9*-regulated signaling phenotypes, our data are compatible with the idea that genetic interactions between the $Nedd9^{-/-}$ and $Pkd1^{-/-}$ genotypes result in morphologically aberrant cilia that cause signaling miscues. These include selective disruption of the ciliary localization of a regulator of cAMP (ACIII), altered Ca^{2+} release in response to exogenous cues, and hyper-activation of SRC, S6, and ERK. These ciliary defects are likely mediated in large part through failure to appropriately activate Aurora-A. Importantly, our analysis showed that treatment of mice with an Aurora-A inhibitor currently in clinical trials exacerbated cyst formation, and also contributed to the formation of misshapen cilia and other phenotypes similar to those seen with the $Nedd9^{-/-}$ genotype. These results provide a potential note of caution as to use of such agents in patients prone to cystogenesis.

At present, studies of the role of cilia in cystic syndromes suggest a bifurcated action dependent on the context of the initiating lesion (36–39). Although loss of cilia due to inactivating mutations in IFT proteins can independently induce cystogenesis, recent strong evidence supports the idea that in the context of lesions in Pkd1 that cause defective signaling from cilia, the removal of cilia suppresses cyst formation (36, 37). Our data are consistent with these results; moreover, although activation of Src, ERK, and mTOR pathway signaling was not found to be necessary for cystogenesis linked to mutation of Pkd1 (36, 37), our work also showed that loss of Nedd9 in the context of a Pkd1 mutation activated these pathways. Although Nedd9 is typically a positive regulator of these proteins, studies of forced oncogene-dependent proliferation of cells in a $Nedd9^{-/-}$ genotype indicate that loss of Nedd9 can cause reflexive hyperactivation of ERK and other proliferative signaling proteins (15). It is also possible that Nedd9 also interacts with additional signaling pathways relevant to ADPKD beyond the set studied here. For instance, one early study indicated that Nedd9 binds directly to the differentiation regulatory protein Id2 (40), which, in turn, has been reported to bind directly to the Pkd2 protein, and mediate proliferative signals in ADPKD (41). Finally, of relevance to the evaluation and treatment of ADPKD families, polymorphisms have been identified in Nedd9 that have been linked with altered protein expression. Studies of these polymorphic variants to date have suggested possible linkage with two neurodegenerative syndromes, Alzheimer's and Parkinson disease, and with atherosclerosis (42–44). Study of variations in Nedd9 expression among individuals potentially will provide a valuable source of insight into the heterogeneous presentation of ADPKD, with this information also serving to guide therapeutic management.

Materials and Methods

Mouse Strains and in Vivo Drug Treatment. The Institutional Animal Care and Use Committee of Fox Chase Cancer Center approved all experiments involving mice. Conditional $Pkd1^{-/-}$ mice in which the Cre-flox regulatory system permits targeted inactivation of the Pkd1 gene in vivo have been described (23, 24). C57BL/6 $Nedd9^{-/-}$ mice were crossed to $Pkd1fl/fl;Cre/Esr1^{+/-}$ to generate $Nedd9^{-/-};Pkd1fl/fl;Cre/Esr1^{+/-}$. $Pkd1fl/fl;Cre/Esr1^{+}$ (referred to as $Pkd1^{-/-}$), $Nedd9^{-/-};Pkd1fl/fl;Cre/Esr1^{+}$ (referred to as $Pkd1^{-/-};Nedd9^{-/-}$), $Nedd9^{-/-};Pkd1fl/fl;Cre/Esr1^{-}$ (referred to as $Nedd9^{-/-}$), and control wild-type ($Pkd1fl/fl;Cre/Esr1^{-}$) mice were injected i.p. with tamoxifen (250 mg/kg body weight, formulated in corn oil) on P2 and P3 for the early cyst induction, or P35 and P36 for late cyst induction, to induce *Pkd1* deletion in the test group, as described (23). Alisertib (MLN8237; Millennium Pharmaceuticals) was formulated in 10% 2-hydroxypropyl-β-cyclodextrin (Sigma-Aldrich) with 1% (vol/vol) sodium bicarbonate and 20 mg/kg administered orally twice daily, using a 5 d on/2 d off schedule. Mice were treated for 8 wk, and cyst growth was monitored by MRI. Treatment began at the age of 4 mo and mice were euthanized 8 wk later to collect kidneys for analysis. Details of MRI procedures and histopathological analysis are provided in *SI Materials and Methods*.

Cells and Cell Culture. Nonimmortalized primary epithelial kidney cells derived from P10 mice (three independent animals per genotype) were maintained in low calcium media containing 5% (vol/vol) chelated horse serum. Only cells between passages 3 and 8 were used for experiments. Cell viability was quantified by using the CellTiter-Blue Assay. Experiments using alisertib and anacardic acid to manipulate cilia in cultured cells are described in *SI Materials and Methods*.

Immunofluorescent analysis was performed by standard protocols (*SI Materials and Methods*). Confocal microscopy was performed by using a confocal microscope (C1 Spectral; Nikon) equipped with an N.A. 1.40 oil immersion 60Å~ Plan Apochromat objective (Nikon). Images were acquired at room temperature (RT) by using EZ-C1 3.8 (Nikon) software and analyzed by using the imaging MetaMorph (Molecular Devices) and Photoshop (version CS5; Adobe) software. Adjustments to brightness and contrast were minimal and were applied to the whole image.

For cytosolic calcium measurement, cells were plated on glass coverslips and grown to ~80% confluence. The coverslips were mounted in a perfusion chamber (FC2; Bioptechs), and analyzed with a microscope (C1 Spectral confocal) equipped with an N.A. 1.40 oil immersion 60Å~ Plan Apochromat objective (Nikon) or an N.A. 1.3 oil immersion 40Å~ Plan Fluo objective (Nikon). Images were acquired by using EZ-C1 3.8 software at RT in HBSS media. Cells were stimulated with 100 nM arginine vasopressin in the absence of extracellular Ca^{2+} on cells washed and assayed in the HBSS free of Ca^{2+} and Mg^{2+}. Fluo-4 was excited at 488 nm, and emission was time-lapse recorded at 522 nm.

Western Blotting. Mouse kidneys were fresh frozen and lysates were prepared for analysis by Western blotting. Western blotting and analysis were performed by standard protocols (*SI Materials and Methods*).

Statistical Analysis. For statistical analyses, we used Wilcoxon rank-sum tests and generalized linear models with appropriate family and link functions (e.g., Gamma or Gaussian families with log or identity links). Where necessary, we estimated growth curves by using generalized estimating equations with exchangeable or Markov working correlation matrices to account for correlated data (for example, Fig. 5*F*) (45). Analyses were performed by using STATA version 12. We tested heterogeneity by comparing the SDs among groups.

ACKNOWLEDGMENTS. We thank Dr. Gregory Germino for the gift of the *Pkd1fl/fl;Cre/Esr1*$^{+/-}$ mice, Simon Tarpinian and Justin Rambert of the Fox Chase Laboratory Animal Facility for help with mice, Emmanuelle Nicolas of the Fox Chase Genomics Facility for help with RT-PCR, and members of the Histopathology Facility. We thank Catherine and Peter Getchell and the Bucks County Chapter of the Fox Chase Board of Associates for their financial support. This work was further supported by funding from National Institutes of Health (NIH) Grant R01 CA63366, Department of Defense Peer Reviewed Medical Research Program Grant W81XWH-12-1-0437/PR110518, and the Fox Chase Kidney Keystone program (to E.A.G.); German Research Foundation Grant SE2280/1 (to T.S-N.); and NIH Core Grant CA06927 (to Fox Chase Cancer Center).

1. Harris PC, Torres VE (2009) Polycystic kidney disease. *Annu Rev Med* 60:321–337.
2. Torres VE, Harris PC (2009) Autosomal dominant polycystic kidney disease: The last 3 years. *Kidney Int* 76(2):149–168.
3. Jonassen JA, San Agustin J, Follit JA, Pazour GJ (2008) Deletion of IFT20 in the mouse kidney causes misorientation of the mitotic spindle and cystic kidney disease. *J Cell Biol* 183(3):377–384.
4. van Seventer GA, et al. (2001) Focal adhesion kinase regulates beta1 integrin-dependent T cell migration through an HEF1 effector pathway. *Eur J Immunol* 31(5): 1417–1427.
5. Fashena SJ, Einarson MB, O'Neill GM, Patriotis C, Golemis EA (2002) Dissection of HEF1-dependent functions in motility and transcriptional regulation. *J Cell Sci* 115(Pt 1): 99–111.
6. O'Neill GM, Golemis EA (2001) Proteolysis of the docking protein HEF1 and implications for focal adhesion dynamics. *Mol Cell Biol* 21(15):5094–5108.
7. Astsaturov I, et al. (2010) Synthetic lethal screen of an EGFR-centered network to improve targeted therapies. *Sci Signal* 3(140):ra67.
8. Izumchenko E, et al. (2009) NEDD9 promotes oncogenic signaling in mammary tumor development. *Cancer Res* 69(18):7198–7206.
9. Pugacheva EN, Roegiers F, Golemis EA (2006) Interdependence of cell attachment and cell cycle signaling. *Curr Opin Cell Biol* 18(5):507–515.
10. Singh MK, et al. (2008) A novel Cas family member, HEPL, regulates FAK and cell spreading. *Mol Biol Cell* 19(4):1627–1636.
11. Plotnikova OV, Golemis EA, Pugacheva EN (2008) Cell cycle-dependent ciliogenesis and cancer. *Cancer Res* 68(7):2058–2061.
12. Pugacheva EN, Jablonski SA, Hartman TR, Henske EP, Golemis EA (2007) HEF1-dependent Aurora A activation induces disassembly of the primary cilium. *Cell* 129(7): 1351–1363.
13. Little JL, et al. (2014) A requirement for Nedd9 in luminal progenitor cells prior to mammary tumorigenesis in MMTV-HER2/ErbB2 mice. *Oncogene* 33(4):411–420.
14. Seo S, et al. (2011) Crk-associated substrate lymphocyte type regulates myeloid cell motility and suppresses the progression of leukemia induced by p210Bcr/Abl. *Cancer Sci* 102(12):2109–2117.
15. Singh MK, et al. (2010) Enhanced genetic instability and dasatinib sensitivity in mammary tumor cells lacking NEDD9. *Cancer Res* 70(21):8907–8916.
16. Tikhmyanova N, Golemis EA (2011) NEDD9 and BCAR1 negatively regulate E-cadherin membrane localization, and promote E-cadherin degradation. *PLoS ONE* 6(7):e22102.
17. Tikhmyanova N, Tulin AV, Roegiers F, Golemis EA (2010) Dcas supports cell polarization and cell-cell adhesion complexes in development. *PLoS ONE* 5(8):e12369.
18. Pugacheva EN, Golemis EA (2005) The focal adhesion scaffolding protein HEF1 regulates activation of the Aurora-A and Nek2 kinases at the centrosome. *Nat Cell Biol* 7(10):937–946.
19. Pugacheva EN, Golemis EA (2006) HEF1-aurora A interactions: Points of dialog between the cell cycle and cell attachment signaling networks. *Cell Cycle* 5(4):384–391.
20. Plotnikova OV, Pugacheva EN, Golemis EA (2011) Aurora A kinase activity influences calcium signaling in kidney cells. *J Cell Biol* 193(6):1021–1032.
21. Plotnikova OV, Pugacheva EN, Dunbrack RL, Golemis EA (2010) Rapid calcium-dependent activation of Aurora-A kinase. *Nat Commun* 1:64.
22. Foggensteiner L, et al. (2000) Cellular and subcellular distribution of polycystin-2, the protein product of the PKD2 gene. *J Am Soc Nephrol* 11(5):814–827.
23. Piontek K, Menezes LF, Garcia-Gonzalez MA, Huso DL, Germino GG (2007) A critical developmental switch defines the kinetics of kidney cyst formation after loss of Pkd1. *Nat Med* 13(12):1490–1495.
24. Piontek KB, et al. (2004) A functional floxed allele of Pkd1 that can be conditionally inactivated in vivo. *J Am Soc Nephrol* 15(12):3035–3043.
25. Seo S, et al. (2005) Crk-associated substrate lymphocyte type is required for lymphocyte trafficking and marginal zone B cell maintenance. *J Immunol* 175(6): 3492–3501.
26. Pazour GJ, et al. (2000) Chlamydomonas IFT88 and its mouse homologue, polycystic kidney disease gene tg737, are required for assembly of cilia and flagella. *J Cell Biol* 151(3):709–718.
27. Humbert MC, et al. (2012) ARL13B, PDE6D, and CEP164 form a functional network for INPP5E ciliary targeting. *Proc Natl Acad Sci USA* 109(48):19691–19696.
28. Pinto CS, Reif GA, Nivens E, White C, Wallace DP (2012) Calmodulin-sensitive adenylyl cyclases mediate AVP-dependent cAMP production and Cl- secretion by human autosomal dominant polycystic kidney cells. *Am J Physiol Renal Physiol* 303(10): F1412–F1424.
29. Halbritter J, et al.; UK10K Consortium (2013) Defects in the IFT-B component IFT172 cause Jeune and Mainzer-Saldino syndromes in humans. *Am J Hum Genet* 93(5): 915–925.
30. Saigusa T, et al. (2012) Collecting duct cells that lack normal cilia have mislocalized vasopressin-2 receptors. *Am J Physiol Renal Physiol* 302(7):F801–F808.
31. Plotnikova OV, et al. (2012) Calmodulin activation of Aurora-A kinase (AURKA) is required during ciliary disassembly and in mitosis. *Mol Biol Cell* 23(14):2658–2670.
32. Ratushny V, et al. (2012) Dual inhibition of SRC and Aurora kinases induces post-mitotic attachment defects and cell death. *Oncogene* 31(10):1217–1227.
33. Law SF, Zhang Y-Z, Klein-Szanto AJ, Golemis EA (1998) Cell cycle-regulated processing of HEF1 to multiple protein forms differentially targeted to multiple subcellular compartments. *Mol Cell Biol* 18(6):3540–3551.
34. Kishore AH, et al. (2008) Specific small-molecule activator of Aurora kinase A induces autophosphorylation in a cell-free system. *J Med Chem* 51(4):792–797.
35. Tikhmyanova N, Little JL, Golemis EA (2010) CAS proteins in normal and pathological cell growth control. *Cell Mol Life Sci* 67(7):1025–1048.
36. Ma M, Tian X, Igarashi P, Pazour GJ, Somlo S (2013) Loss of cilia suppresses cyst growth in genetic models of autosomal dominant polycystic kidney disease. *Nat Genet* 45(9): 1004–1012.
37. Sharma N, et al. (2013) Proximal tubule proliferation is insufficient to induce rapid cyst formation after cilia disruption. *J Am Soc Nephrol* 24(3):456–464.
38. Cadieux C, et al. (2008) Polycystic kidneys caused by sustained expression of Cux1 isoform p75. *J Biol Chem* 283(20):13817–13824.
39. Tammachote R, et al. (2009) Ciliary and centrosomal defects associated with mutation and depletion of the Meckel syndrome genes MKS1 and MKS3. *Hum Mol Genet* 18(17):3311–3323.
40. Law SF, et al. (1999) Dimerization of the docking/adaptor protein HEF1 via a carboxy-terminal helix-loop-helix domain. *Exp Cell Res* 252(1):224–235.
41. Li X, et al. (2005) Polycystin-1 and polycystin-2 regulate the cell cycle through the helix-loop-helix inhibitor Id2. *Nat Cell Biol* 7(12):1202–1212.
42. Ma L, Clark AG, Keinan A (2013) Gene-based testing of interactions in association studies of quantitative traits. *PLoS Genet* 9(2):e1003321.
43. Li Y, et al. (2008) Evidence that common variation in NEDD9 is associated with susceptibility to late-onset Alzheimer's and Parkinson's disease. *Hum Mol Genet* 17(5): 759–767.
44. Wang Y, et al. (2012) NEDD9 rs760678 polymorphism and the risk of Alzheimer's disease: A meta-analysis. *Neurosci Lett* 527(2):121–125.
45. Shults J, Ratcliffe SJ, Leonard M (2007) Improved generalized estimating equation analysis via xtqls for implementation of quasi-least squares in STATA. *Stata J* 7(2):147–166.